THE JOURNAL OF PHYSICAL CHEMISTRY B

ARTICLE

pubs.acs.org/JPCB

Hydration of Formate and Acetate Ions by Dielectric Relaxation Spectroscopy

Hafiz M. A. Rahman,[†] Glenn Hefter,[‡] and Richard Buchner*[,†]

[†]Institut für Physikalische und Theoretische Chemie, Universität Regensburg, D-93040 Regensburg, Germany

[‡]Chemistry Department, Murdoch University, Murdoch, WA 6150, Australia

Supporting Information

ABSTRACT:

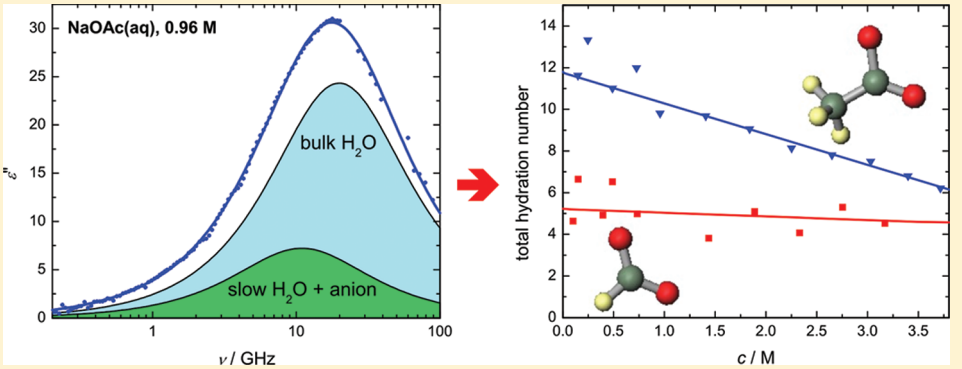

Dielectric relaxation (DR) spectra have been measured for aqueous solutions of sodium formate (NaOFm) and sodium acetate (NaOAc) over a wide range of frequencies ($0.2 \leq \nu/\mathrm{GHz} \leq 89$) up to solute concentrations $c \lesssim 3.2$ M and $\lesssim 3.7$ M, respectively, at 25 °C. Measurements were also made on NaOAc(aq) at $15 \leq T/°\mathrm{C} \leq 35$. In addition to the usual dominant bulk-water relaxation process at ~20 GHz, one or two further relaxation modes were detected. One process, centered at ~8 GHz and observed for both NaOFm(aq) and NaOAc(aq), was attributed to the presence of slow water in the hydration shells of the anions. A lower-frequency process at ~0.6 GHz, observed only for NaOAc(aq) at $c \lesssim 1$ M, was thought to be due to the presence of very small concentrations of ion pairs. Detailed analysis of the spectra indicated that very few (<2 per anion) water molecules were irrotationally bound (frozen) on the DR time scale. Nevertheless, both anions are strongly hydrated, as evidenced by the significant amounts of slow water detected. Such H_2O molecules with reduced dynamics result from two distinct effects. The first is the relatively strong hydrophilic interaction of water with the $-COO^-$ moiety, which is similar for the two anions and little affected by increasing solute concentration. The second (for OAc^- only) is the hydrophobic hydration of the $-CH_3$ group, which is fragile, decreasing markedly with increasing solute concentration and temperature. The activation parameters for bulk-water relaxation in NaOAc(aq) indicated a breakdown of the bulk water structure at high solute concentrations.

1. INTRODUCTION

Solute−solvent interactions are of critical importance in physical, environmental, and surface chemistry.[1] Knowledge of the nature of ion hydration is especially important in biology because it is a prerequisite for understanding the processes occurring in living cells.[1] For example, proteins and other biomolecules have evolved to function optimally in particular aqueous environments for which specific patterns of hydrophobic and hydrophilic components at their surface are believed to be essential.[1] Furthermore, biomolecules are known to influence their surrounding solvent layers, and this effect is reciprocal in that the solvent modifies the structure and activity of the biomolecules. Investigation of biomolecule hydration, especially of proteins, has a long tradition.[1−4] However, quantitative interpretation of the observed behavior is often problematic, even when using the popular NMR techniques,[5] because of the similarity of the time-scales of H_2O dynamics in the vicinity of solute species and in the bulk solvent.

A common approach to get around these difficulties is to study smaller model compounds, such as amino acids or low-molecular-mass peptides, which contain key structural and/or chemical features of the larger species. Such molecules are of a size that is within the reach of computer simulations[6,7] and scattering methods.[8,9] Dielectric relaxation spectroscopy (DRS), which probes the response of dipolar species to a time-dependent electric field in the microwave region, is a particularly powerful tool for such studies

Received: August 5, 2011
Revised: October 20, 2011
Published: November 18, 2011

because it provides quantitative information on the cooperative dynamics of both solute and solvent species.[10,11]

As already noted, an important feature of the hydration of many biomolecules is the close proximity of hydrophobic and hydrophilic moieties at their surfaces. However, the interaction of these disparate entities and their surrounding water molecules is not well understood. Carboxylate ($-COO^-$) groups are the major anionic sites in most biomolecules, being present, for example, in amino acids, fatty acids, lipid bilayers, and surface-active agents.[12] In addition, the active sites of enzymes often feature carboxylate groups to facilitate metal-ion binding.[13]

This article presents a detailed DRS study of the aqueous solutions of the two simplest carboxylate ions: methanoate ($HCOO^-$, formate, OFm^-) and ethanoate (CH_3COO^-, acetate, OAc^-), as their sodium salts. Carboxylate concentrations were investigated up to ~3.2 M (OFm^-) or ~3.7 M (OAc^-) over the frequency range $0.2 \lesssim \nu/\mathrm{GHz} \leq 89$ in order to develop an overview of the hydration characteristics of these two model ions. To the best of our knowledge, only a few previous DRS studies of the aqueous solutions of carboxylate salts have been reported. Of particular note are those of Lyashchenko et al.,[14−16] which showed that the bulk water relaxation time decreased with increasing formate concentration, whereas in propanoate solutions, it increased. This difference was interpreted[15] as indicating that OFm^- is hydrophilic, whereas propanoate is hydrophobic. Unfortunately, because of technological limitations (data were obtained at just seven frequencies between 7 and 25 GHz at $c \gtrsim 0.5$ M),[14−16] no further significant conclusions could be drawn by the authors at that time. The present article, thus, represents a significant extension of the DRS database for these important ions.

2. EXPERIMENTAL SECTION

Sodium formate (NaOFm, purity ≥99%) and sodium acetate (NaOAc, purity 99%) were obtained from Merck (Germany) and Alfa Aesar (Germany), respectively. Both salts were dried at 50 °C under vacuum (~ 10^{-5} bar) for at least 72 h using P_2O_5 (Sicapent, Merck) as a desiccant and were subsequently stored in a nitrogen filled glovebox prior to use. Solutions were prepared gravimetrically without buoyancy corrections using degassed Millipore MILLI-Q water. However, for data processing purposes, all solute concentrations, c, are expressed in M, (mol-solute/L-solution). Solution densities, ρ, required for the interconversion, were measured with an accuracy of ±0.05 kg m^{-3} using a vibrating-tube densimeter (Anton Paar DMA 60/601HT) calibrated with N_2(g) and water, assuming densities from standard sources.[17]

Electrical conductivities of the solutions, κ, were measured with an accuracy of ±0.5% using the equipment described previously.[18] A set of five two-electrode capillary cells with cell constants, C, in the range of 25 to 360 cm^{-1} was used. The cells were calibrated with aqueous solutions of KCl.[18] The cell resistance, $R(\nu)$, was measured with a manual high-precision conductivity bridge as a function of the applied AC frequency, ν, between 120 Hz and 10 kHz. To eliminate electrode polarization contributions, the conductivity of each sample, $\kappa = C/R_\infty$, where $R_\infty = \lim_{\nu\to\infty} R(\nu)$, was obtained by extrapolation using the empirical function $R(\nu) = R_\infty + A/\nu^a$, where A is specific to each cell, and $a \approx 0.5$.[18] The data for ρ and κ are included in Tables S1 and S2 of the Supporting Information.

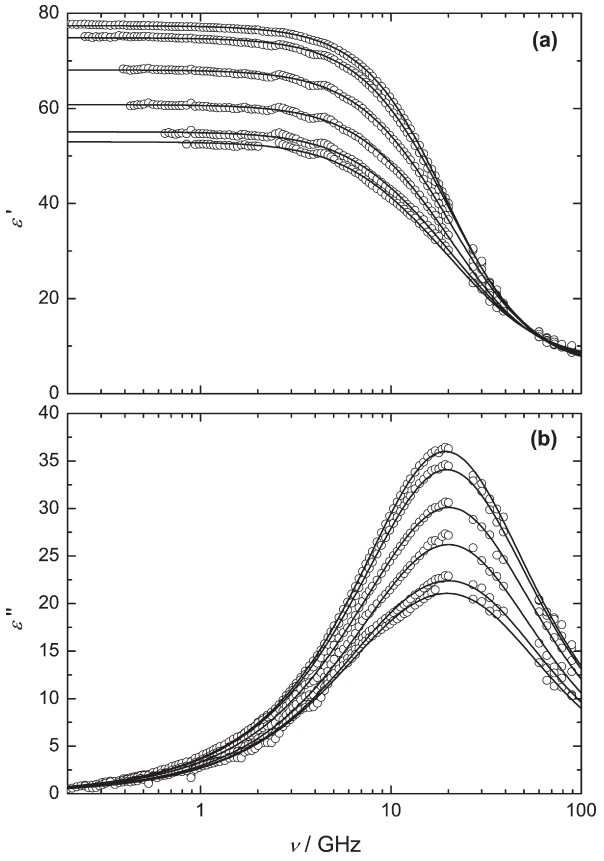

Figure 1. Permittivity, $\varepsilon'(\nu)$ (a), and dielectric loss, $\varepsilon''(\nu)$ (b), spectra for NaOFm(aq) at 25 °C and concentrations c (M) = 0.07469, 0.2968, 0.9617, 1.888, 2.753, and 3.171 (top to bottom). Symbols show experimental data; lines represent the D + D fit.

Dielectric spectra of aqueous solutions of NaOFm at 25 °C and of aqueous NaOAc solutions at 15, 25, and 35 °C were recorded in the frequency range $\nu_{\min} \leq \nu/\mathrm{GHz} \leq 20$ at Murdoch University using a Hewlett-Packard model 85070 M dielectric probe system based on a HP 8720D vector network analyzer (VNA) as described previously.[19] The temperature was controlled by a Hetofrig (Denmark) circulator-thermostat with a precision of ±0.02 °C and an accuracy (NIST-traceable) of ±0.05 °C. The value of the minimum accessible frequency, $\nu_{\min}$, was determined by the conductivity contribution to the loss spectrum. As such, it varied with concentration and solute but was typically in the range of 0.2 to 0.8 GHz. All VNA spectra were recorded at least twice using independent calibrations with air, water, and mercury as the references.[19] Higher frequency data were recorded at Regensburg using two waveguide interferometers (IFMs) covering the ranges of $27 \leq \nu/\mathrm{GHz} \leq 39$ and $60 \leq \nu/\mathrm{GHz} \leq 89$. The operation of the IFMs, which do not require calibration, is described in detail elsewhere.[20] Temperature control and accuracy were similar to those at Murdoch. Typical spectra and the corresponding fits are shown in Figure 1, as well as in Figures S1−S4 of the Supporting Information.

3. DATA ANALYSIS

Dielectric spectroscopy records the total polarization, $\vec{P}(t)$, of a sample in a time-dependent field, $\vec{E}(t)$.[21,22] This response is usually expressed as a function of the field frequency, ν, in terms

of the complex permittivity

$$\hat{\varepsilon}(\nu) = \varepsilon'(\nu) - i\varepsilon''(\nu) \quad (1)$$

The relative permittivity, $\varepsilon'(\nu)$, exhibits a dispersion ranging from the static permittivity limit, ε, at $\nu \rightarrow 0$ to the high-frequency limit, ε_∞. The dielectric loss, $\varepsilon''(\nu)$, expresses the energy dissipation within the sample, arising from the coupling of $\vec{E}(t)$ to dipole fluctuations. For electrically conducting samples of dc conductivity, κ, charge transport creates an additional Ohmic loss term. Since only the total loss, $\eta''(\nu)$, is experimentally accessible, the dielectric loss, $\varepsilon''(\nu)$, must be obtained by correcting for this effect[23] by assuming

$$\varepsilon''(\nu) = \eta''(\nu) + \frac{\kappa}{2\pi\nu\varepsilon_0} \quad (2)$$

where ε_0 is the permittivity of free space.[21] To obtain $\varepsilon''(\nu)$, the experimental total loss curve for each VNA spectrum was analyzed separately via eq 2 to determine the slightly calibration-dependent conductivity at each concentration.[19] The resulting κ values were generally 1−2% smaller than conventional (low frequency) conductivity data, with deviations becoming slightly larger at high electrolyte concentrations. Provided the agreement of κ values obtained was better than ±2% for at least two measurements, the averaged VNA spectra were combined with interferometer data. For the latter, the experimental conductivities of Tables S1 and S2 (Supporting Information) were used to calculate $\varepsilon''(\nu)$ from $\eta''(\nu)$. There was, in general, a smooth connection between the low and high frequency data (Figures 1 and S1−S4, Supporting Information), although, as is usually observed for electrolyte solutions, the noise increased with increasing solute concentration (conductivity) due to the increasing difference between the dielectric properties of the reference liquid (water) and of the sample.[19] Electrode polarization was negligible for all samples as none of the $\varepsilon'(\nu)$ spectra showed the typical power-law rise with decreasing frequency that would indicate the presence of significant polarization.[22]

The combined $\hat{\varepsilon}(\nu)$ data were analyzed by simultaneously fitting the in-phase ($\varepsilon'(\nu)$; Figures 1a and S1a−S4a, Supporting Information) and out-of-phase ($\varepsilon''(\nu)$; Figures 1b and S1b−S4b, Supporting Information) components of the complex permittivity to various possible relaxation models consisting of n distinguishable relaxation processes[10,11]

$$\hat{\varepsilon}(\nu) = \varepsilon_\infty + \sum_{j=1}^{n} \frac{\varepsilon_j - \varepsilon_{j+1}}{(1 + (i2\pi\nu\tau_j)^{1-\alpha_j})^{\beta_j}} \quad (3)$$

with each dispersion step j, of amplitude $S_j = \varepsilon_j - \varepsilon_{j+1}$ and relaxation time τ_j, being modeled using a Havriliak−Negami (HN) equation with relaxation-time distribution parameters $0 < \alpha_j < 1$ and $0 < \beta_j \leq 1$. Simplified variants of this equation correspond to the Cole−Davidson (CD, $\alpha_j = 0$), Cole−Cole (CC, $\beta_j = 1$), and Debye (D, $\alpha_j = 0, \beta_j = 1$) models.[21] Other band shape functions more appropriate for intermolecular vibrations and librations, such as damped harmonic oscillators, were not considered as such modes make negligible contributions to the dielectric spectra of aqueous systems at gigahertz frequencies.[24] The fitting program developed in our laboratory uses Bevington's[25] CURFIT routine extended to complex numbers, which is based on the Marquart algorithm. The quality of the fit was evaluated via the reduced error function, χ_r^2.[25] Following the decision criteria outlined in detail elsewhere,[26] the model adopted was that which gave the lowest value of χ_r^2 and

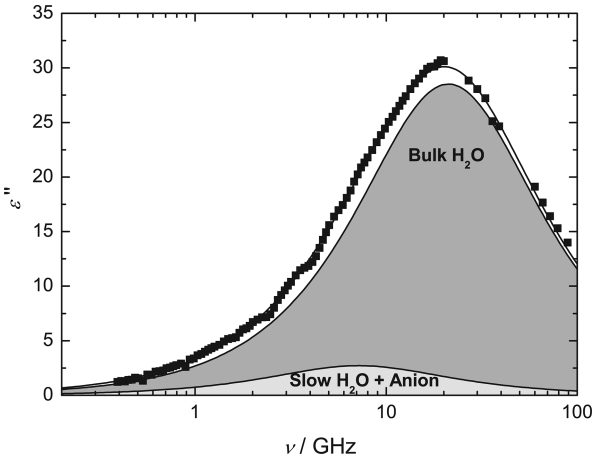

Figure 2. Dielectric loss spectrum, $\varepsilon''(\nu)$, of 0.9617 M NaOFm(aq) at 25 °C. Symbols represent experimental data, the line represents the D + D fit, and shaded areas indicate the contributions of the two relaxation modes.

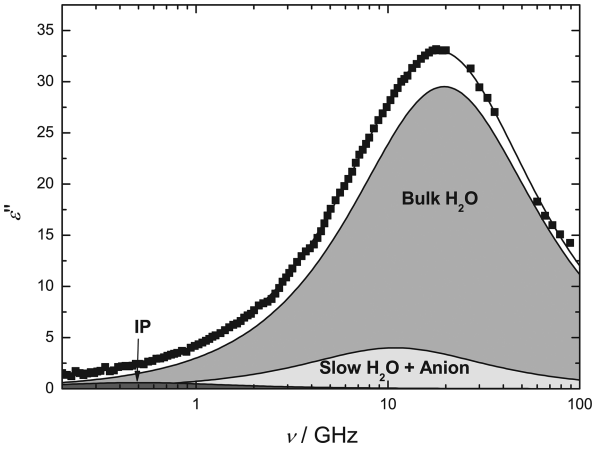

Figure 3. Dielectric loss spectrum, $\varepsilon''(\nu)$, of 0.4881 M NaOAc(aq) at 25 °C. Symbols represent experimental data, the line represents the D + D + D fit, and shaded areas indicate the contributions of the three relaxation modes.

relaxation amplitudes and times that were physically realistic and which varied smoothly with solute concentration. Additionally, selected spectra were analyzed using a recently published procedure[27] that allows an unbiased determination of the number of relaxation processes required for formal description of the observed $\hat{\varepsilon}(\nu)$ data. These results fully confirmed the fit model selected with our standard procedure[26] on the basis of eq 3.

In eq 3, $\varepsilon_\infty = \varepsilon_{n+1}$ is the so-called infinite-frequency permittivity, which in principle reflects contributions only from intramolecular polarizability. Accurate determination of ε_∞ requires experiments at far-infrared frequencies where contributions from molecular librations become negligible.[21,24] However, this part of the spectrum is difficult to access experimentally, and ε_∞ was, therefore, treated as an adjustable parameter. For some calculations (section 4.2), ε_∞ was assumed to be the same as for pure water. The static relative permittivity of the sample is defined as $\varepsilon = \varepsilon_1 = \Sigma S_j + \varepsilon_\infty$. All fitting parameters obtained from the present spectra are summarized in Tables S1 and S2 of the Supporting Information.

4. RESULTS AND DISCUSSION

4.1. Assignment of Relaxation Modes. Representative dielectric spectra measured for NaOFm(aq) as a function of concentration are shown in Figure 1; those for NaOAc(aq) at 15, 25, and 35 °C are given in Figures S1 to S4 of the Supporting Information. Overall, the spectra were best described by a model consisting of either two (for NaOFm(aq) at all c and for NaOAc(aq) at $c > 1$ M) or three (for NaOAc(aq) at $c \lesssim 1$ M) Debye processes. Typical fits obtained with these D + D and D + D + D models are shown in Figures 2 and 3. These models were consistent with the bias-free analysis of the spectra shown in Figures S5 amd S6 of the Supporting Information.

As is usual for aqueous electrolyte solutions, the spectra for the solutions of both salts were dominated by the cooperative relaxation of bulk water, readily identified by its location (~20 GHz) and magnitude. In addition, the relaxation times for this mode, τ_b (= τ_2 for NaOFm(aq) in Table S1; τ_3 for NaOAc(aq) in Table S2 of the Supporting Information), extrapolate smoothly to the pure water values, $\tau_b(0)$, of 10.8, 8.32, and 6.53 ps at 15, 25, and 35 °C, respectively (Figures S7 and S8a, Supporting Information). There is, however, a significant difference between the two sets of salt solutions in that the position of the experimentally observed loss peak is almost invariant with c for NaOFm(aq) (Figure 1b), whereas for NaOAc(aq) it shifts to much lower frequencies and becomes clearly asymmetric with increasing c (Figures S1b to S3b, Supporting Information).

Detailed analysis indicated that these changes were due to the presence of another mode, centered at ~8 GHz, whose intensity increased considerably, relative to the decreasing bulk-water amplitude, with increasing solute concentration. Broadly consistent with an unbiased analysis[27] of the data (Figures S5 and S6, Supporting Information), this mode was also found to be present in the NaOFm(aq) spectra, albeit with a smaller amplitude especially at high c, which did not significantly affect the location of the maximum observed for $\varepsilon''(\nu)$. The average relaxation time[28] of this slower process at 25 °C, $\tau_1 \approx 15$ ps for NaOFm(aq) (Figure S7, Supporting Information), and $\tau_2 \approx 16$ ps for NaOAc(aq) (Figure S8b, Supporting Information), is almost twice that of the bulk water mode ($\tau_b \approx 8$ ps) but similar to the relaxation times observed for slow water molecules involved in the hydration of either hydrophobic solutes[29,30] or moderately hydrophilic anions.[31−33] Accordingly, this mode is tentatively assigned to the presence of slow water molecules. However, it must be remembered that both OFm^- and OAc^- have dipole moments (the gas phase values of μ_- are 1.40 and 3.64 D, respectively[34]). Since DRS is sensitive to all dipolar species,[11] both ions will contribute to the spectra. As no separate relaxation process was observed for either anion, it is likely that the relaxation associated with their reorientation, which would be expected to occur at ~5−10 GHz, is subsumed in the slow-water mode. This mode (process 1 for NaOFm(aq) and process 2 for NaOAc(aq)) will, therefore, be referred to from here on as a composite mode.

The detection of an additional low-frequency low-amplitude Debye relaxation, centered at ~0.6 GHz, for NaOAc(aq) at $c \lesssim 1$ M at all temperatures (Figures 3 and S6, Supporting Information) is consistent, from its location and amplitude, with the presence of small amounts of ion-pairs. There were slight indications (Figure S5a, Supporting Information) that such species may also be present in NaOFm(aq), but the scatter in the data and the limited extent of formation precluded quantification. The presence of very weak ion pairing between $Na^+(aq)$ and both $OFm^-(aq)$ and $OAc^-(aq)$ is consistent with thermodynamic data, recent conductivity measurements,[35] and molecular dynamics (MD) simulations.[36]

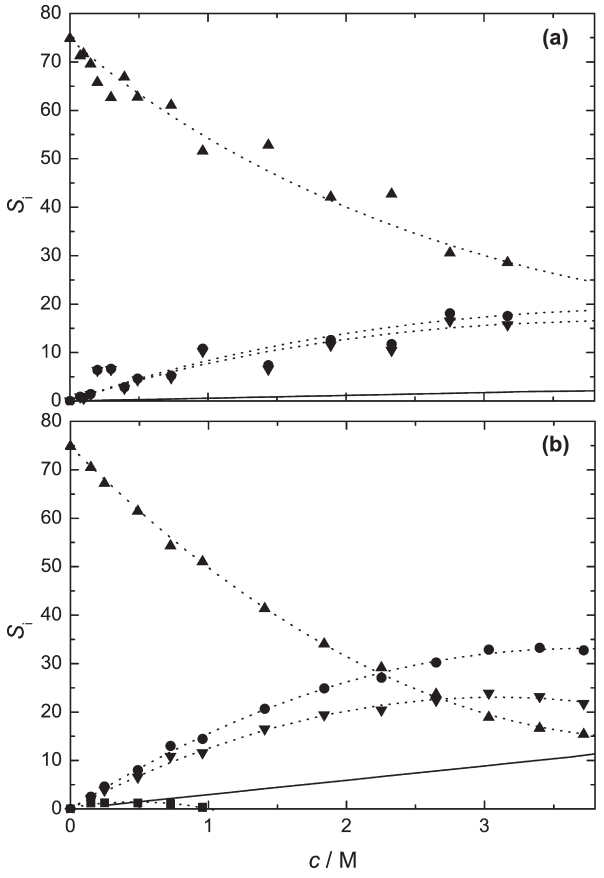

Figure 4. Concentration dependence for (a) NaOFm(aq) and (b) NaOAc(aq) at 25 °C of the relaxation amplitudes of bulk water, S_b (▲), the composite mode, $S_s + S_-$ (●), slow water, S_s (▼), and (NaOAc(aq) only) ion pairs S_{IP} (■). The solid lines represent S_-, calculated via eq 5; the dotted lines are included only as a visual guide.

It is interesting to note that the present spectra, limited to $\nu \leq 89$ GHz, did not produce any evidence for the very fast water process centered at ~400 GHz,[24] which is sometimes,[29,30] but not always,[31] detected in aqueous electrolyte solutions. This absence was consistent with the bias-free simulations (Figures S5 and S6, Supporting Information). Nevertheless, the fitted values of $\varepsilon_\infty \approx 5-7$ (Tables S1 and S2, Supporting Information) are considerably larger than the $\varepsilon_\infty = 3.48$ obtained for pure water,[24,37] which suggests that the fast water process is still making a minor, if unresolvable, contribution to the present spectra.

4.2. Relaxation Amplitudes. *4.2.1. Ion-Pairs.* For NaOAc(aq), the ion-pair relaxation amplitude, $S_{IP} = \varepsilon(c) - \varepsilon_2(c)$, and therefore the ion-pair concentration, passes through a maximum at $c \approx 0.5$ M (Figure 4b). The decrease in S_{IP} at $c > 0.5$ M is consistent with the so-called redissociation that often occurs for weak ion pairs at high salt concentrations.[29,32] However, because S_{IP} is small, with significant scatter, a detailed analysis of the ion-pair mode is not appropriate. As already noted, the presence of ion pairs in NaOAc(aq) is supported by MD simulations[36] and conductivity measurements.[35] No direct potentiometric measurements of ion pairing between $Na^+(aq)$ and $OAc^-(aq)$ appear to have been reported but additional support for their

dx.doi.org/10.1021/jp207504d | J. Phys. Chem. B 2012, 116, 314–323

existence comes from measurements of the association constant (K_A) of acetic acid in different media. Applying an equation analogous to that derived by Hefter[38] to the K_A(HOAc) values reported by Partanen in KCl and NaCl media[39] gave a value of K_A(NaOAc) ≈ 0.07 M^{-1}, corresponding to the equilibrium

$$Na^+(aq) + OAc^-(aq) \rightleftharpoons NaOAc^0(aq) \quad (4)$$

at an ionic strength $I \approx 1$ M (KCl). A similar result was obtained for K_A(NaOFm) using the analogous data for formic acid.[39] Such small K_A values are at the detection limit of the present DRS instrumentation.

4.2.2. Bulk Water. As shown previously,[29] the bulk and (unresolved) fast relaxations for water (at ∼20 GHz and ∼400 GHz, respectively) can be treated collectively by assuming that $S_b = \varepsilon_j(c) - \varepsilon_\infty$, where $j = 2$ for NaOFm(aq) and $j = 3$ for NaOAc(aq). For these calculations, the value of ε_∞ was taken to be that obtained from ultrahigh-frequency dielectric measurements (including THz data[37]) of pure water, rather than the less accurate values derived from fitting the present spectra at $\nu \leq 89$ GHz (Tables S1 and S2, Supporting Information). As can be seen (Figure 4), the magnitude of S_b decreases significantly with increasing c.

Dipole concentrations, c_i, corresponding to relaxation amplitudes, S_i, can be calculated via the generalized Cavell equation[40]

$$c_i(c) = \frac{2\varepsilon(c) + 1}{\varepsilon(c)} \times \frac{k_B T \varepsilon_0}{N_A} \times \frac{(1 - \alpha_i f_i(c))^2}{\mu_i^2} \times S_i(c) \quad (5)$$

where N_A and k_B are the Avogadro and Boltzmann constants, T is the thermodynamic temperature, and ε is the static permittivity. The dipole moment, μ_i, polarizability, α_i, and reaction field factor, f_i, are characteristic of the relaxing species, i.[40]

For evaluation of the bulk water amplitude, it is advantageous to normalize eq 5 to pure water.[26,29] Additionally, for electrolyte solutions, S_b has to be corrected for the kinetic depolarization (kd) that arises from the relative motions of the ions and the surrounding solvent molecules in the external field.[41] Thus, the equilibrium amplitude of the overall solvent relaxation process, $S_b^{eq}(c)$, to be inserted into eq 5 is given by

$$S_b^{eq}(c) = S_b(c) + \Delta_{kd}\varepsilon(c) \quad (6)$$

where

$$\Delta_{kd}\varepsilon(c) = \xi\kappa(c) \quad (7)$$

and

$$\xi = p \times \frac{\varepsilon(0) - \varepsilon_\infty(0)}{\varepsilon(0)} \times \frac{\tau(0)}{\varepsilon_0} \quad (8)$$

In eq 7, $\varepsilon(0)$ is the (relative static) permittivity of pure water and $\tau(0)$ is the relaxation time of its dominant dispersion step.[41] The hydrodynamic parameter p characterizes the translational motion of the ions, with $p = 1$ for stick and $p = 2/3$ for slip boundary conditions; $p = 0$ defines negligible kd. For the present systems, slip boundary conditions were used for calculating the apparent bulk water concentrations, $c_b^{ap}(c)$, as they are considered to be the most physically realistic for the dielectric relaxation of solvated ions.[11,19,26,29]

4.2.3. Composite Process. Figure 4 shows that the amplitude of the composite relaxation mode, $S_{comp} = \varepsilon_j(c) - \varepsilon_{j+1}(c)$, where $j = 1$ for NaOFm(aq) and $j = 2$ for NaOAc(aq), increases with increasing c for both sets of salt solutions, with the magnitude of the latter being somewhat larger. One reason for this is the larger contribution from the higher dipole moment of OAc^-, cf., OFm^-.

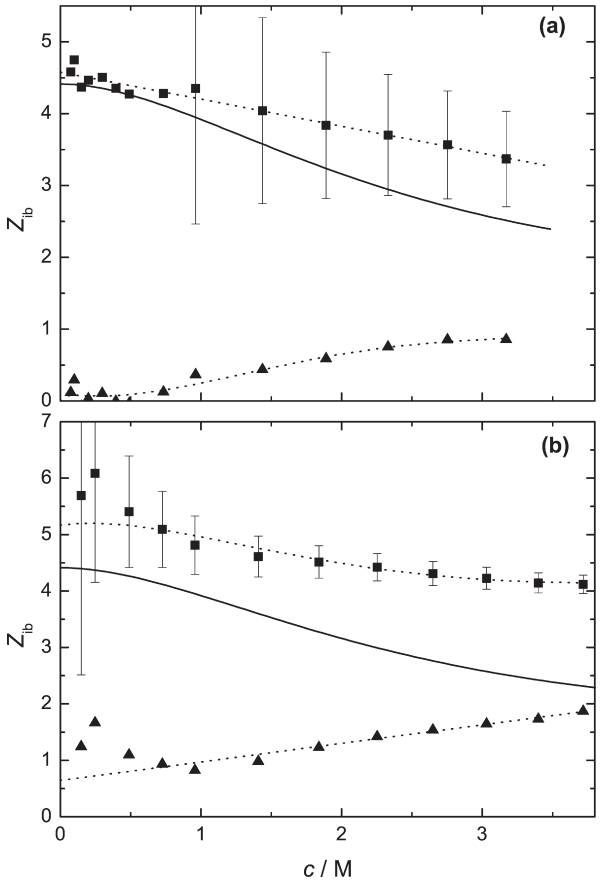

Figure 5. Concentration dependence of effective hydration numbers, Z_{ib}, at 25 °C for (a) NaOFm(aq) (■) and OFm^-(aq) (▲); and (b) NaOAc(aq) (■) and OAc^-(aq) (▲).[70] Solid lines represent $Z_{ib}(Na^+)$; dotted lines are included only as a visual guide.

The amplitude S_{comp} can be split into its constituent relaxation amplitudes as

$$S_{comp} = S_- + S_s \quad (9)$$

where S_- is the relaxation amplitude due to the rotation of the dipolar carboxylate anions, and S_s is the relaxation amplitude of the slow water molecules hydrating the anion. Since ion pairing is weak for the present systems, the magnitude of S_- for OFm^- and OAc^- can be calculated using eq 5. For the effective dipole moments of OFm^- and OAc^- in solution, the ab initio values for $\mu_{eff,-} = \mu_-/(1 - f_-\alpha_-)$, calculated by Serr and Netz,[34] 2.52 and 5.70 D, respectively, were adopted. The amplitude of the slow-water process, S_s, can then be derived via eq 9 from the observed values of S_{comp} and used to calculate the apparent concentration of slow water, $c_s^{ap}(c)$, via eq 5.

Unfortunately, a similar splitting of the composite mode relaxation time, τ_{comp} (τ_1 for NaOFm(aq) and τ_2 for NaOAc(aq)), into those for the anion, τ_-, and for slow water, τ_s, is not possible as it cannot be assumed that the relaxation rates τ_-^{-1} and τ_s^{-1} are independent of concentration and that τ_{comp}^{-1} is their amplitude-weighted average. This is regrettable as it prevents calculation of the activation parameters for slow-water

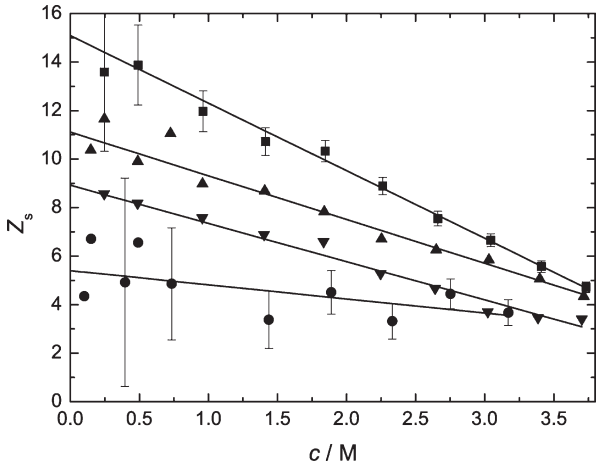

Figure 6. Concentration dependence of the slow-water hydration number, Z_s, for the formate ion in NaOFm(aq) (●) at 25 °C and for the acetate ion in NaOAc(aq) at 15 °C (■); 25 °C (▲); and 35 °C (▼) (error bars[70] were omitted for NaOAc(aq) at 25 °C and 35 °C for visual clarity).

relaxation, which would be of considerable interest (see section 4.5).

4.3. Ion Hydration. For both salts, the strong decrease of S_b (Figure 4) and the emergence of the slow-water process (Figures 2 and 3) with increasing c indicate the presence of strong ion−water interactions. If such interactions are much stronger than water−water interactions, the water molecules bound to the ions effectively become immobilized (irrotationally bound, ib) or frozen on the DRS time scale.

For the present systems, the sum of the DRS-detected c_b^{ap} and c_s^{ap} (section 4.2) is less than the analytical total water concentration, c_w. Water missing from the DR spectrum can be ascribed to the presence of ib water molecules and an effective hydration number, Z_{ib}, can then be defined as the number of such immobilized molecules per unit of dissolved salt

$$Z_{ib} = (c_w - c_b^{ap} - c_s^{ap})/c \quad (10)$$

In contrast, the values of $c_s^{ap}(c)$ obtained from S_s with eq 5 can be used directly to calculate the effective number of slow water molecules per unit of dissolved salt

$$Z_s = c_s^{ap}(c)/c \quad (11)$$

The Z_{ib} values calculated in this way for NaOFm(aq) and NaOAc(aq) at 25 °C are given in Figure 5. To partition these values into their more interesting ionic components, $Z_{ib}(Na^+)$ was obtained from a reanalysis of the 25 °C data for NaCl(aq)[19] with eq 5, along with the assumption of ionic additivity.[42] Note that all the ionic values are ultimately based on the assumption that $Z_{ib}(Cl^-) = 0$ at all temperatures. The Z_{ib} values obtained for OFm^- and OAc^- are also shown in Figure 5. At $c \lesssim 0.75$ M, OFm^- does not appear to irrotationally bind any water molecules (i.e., $Z_{ib}(OFm^-) \approx 0$; Figure 5a), while $Z_{ib}(OAc^-) \approx 1$ (Figure 5b). At $c \gtrsim 1$ M, Z_{ib} for both anions increases slightly with increasing c. This is unusual: most ions studied to date show a decrease in Z_{ib} with increasing c,[10,43] which is thought to be due to increasing overlap of their hydration shells. A possible explanation of this unusual increase might be that some water molecules are held more tightly by bonding simultaneously to both the cation and anion, i.e., as intervening solvent molecules in solvent-separated ion pairs (SIPs). Despite fast redissociation (and thus no detectable SIP relaxation process[11]), such configurations may become frequent at $c \gtrsim 1$ M because of steric crowding.

The Z_s values calculated for NaOFm(aq) and NaOAc(aq) are shown in Figure 6. Since aqueous solutions of common inorganic salts containing Na^+ do not show any slow water process,[43,44] it is reasonable to assign Z_s for both of the present systems to the anions alone. On this basis, the Z_s value for OFm^-(aq) at infinite dilution is ∼5.2 and decreases linearly with increasing c (Figure 6). As OFm^- does not contain a hydrophobic part, these water molecules can reasonably be assumed to be H-bonded to the hydrophilic $-COO^-$ moiety. In line with recent MD simulations,[45] it is postulated that the strength of these H-bonds is greater than that of the water−water H-bonds, thereby slowing their dynamics. This hydrophilic interaction is not strong enough to irrotationally bind these water molecules to the $-COO^-$ moiety since $Z_{ib}(OFm^-) \approx 0$ at $c \to 0$ (Figure 5a). The present assignment accords with recent theoretical investigations by Sterpone et al.,[46] which suggested that the water molecules hydrating the carboxylate group in amino acids are retarded by a factor of ∼2.5 compared to bulk water. They also suggested that, in addition to the stronger $-COO^-\cdots H_2O$ interactions (relative to $H_2O\cdots H_2O$), excluded volume effects are important for slowing the water dynamics. Similarly, Xu and Berne[7] found that H-bond making and breaking kinetics were slower in the first solvation shell of a negatively charged polypeptide, again using MD simulations. Hydrophilically slowed water dynamics have also been observed experimentally for several dicarboxylate ions[32] and F^-.[31,33]

Although the present Z_{ib} values are small ($\lesssim 2$) and should not be overinterpreted given the assumptions involved in obtaining them, it is interesting to note that for OFm^-, the increase of Z_{ib} counterbalances a decrease in Z_s (Figure 6), such that their sum, the total hydration number, is approximately constant ($Z_t \equiv Z_s + Z_{ib} \approx 5$). This implies that the hydration shell of the $-COO^-$ group remains intact, with some variations in bond strength, up to fairly high concentrations. Also, the values of Z_t for the highest OAc^- concentration are roughly independent of the temperature and similar to $Z_t(OFm^-)$. The implications of this finding will be discussed in section 4.4.

Most computer simulations of carboxylate hydration[6,45,47,48] conclude that water is highly structured around the $-COO^-$ group, with an average hydration number of 5−7. However, X-ray and neutron scattering and infrared measurements of concentrated aqueous solutions of sodium and potassium formate[49,50] and acetate[51,52] indicate that the hydration number per $-COO^-$ is <5. NMR studies[53] have suggested there are 5.0−6.5 water molecules around each $-COO^-$ group, while statistical mechanics results suggest that the $-COO^-$ group of OAc^- forms ∼6 H-bonds to adjacent water molecules.[54] Except for refs 49−52, which focus on very concentrated solutions, all these investigations are broadly consistent with the present study (and with each other).

The present results may be compared with those obtained for oxalate ($C_2O_4^{2-}$, ox^{2-}),[55] the simplest of the dicarboxylate anions. At infinite dilution, the total number of water molecules bound to OFm^- (i.e., Z_t) is ∼5.2, which is similar to the value of ∼6 found for $Z_{ib}(ox^{2-})$.[55] As already noted, Z_t remains approximately constant for OFm^- regardless of c. In contrast, the hydration shell of ox^{2-} is particularly fragile, decreasing rapidly with increasing solute concentration such that at 0.25 M, the

dx.doi.org/10.1021/jp207504d | J. Phys. Chem. B 2012, 116, 314–323

highest concentration studied due to the limited solubility of $Na_2ox(s)$, $Z_{ib}(ox^{2-}) \approx 2.3$.[55] The apparent contradiction that $Z_{ib}(ox^{2-}) > Z_{ib}(OFm^-)$ at infinite dilution, yet $Z_{ib}(ox^{2-})$ decreases sharply with increasing c, while $Z_{ib}(OFm^-)$ increases (Figure 5 a), may merely reflect a failure to detect slow water for $Na_2ox(aq)$ due to the limited accessible concentration range. In this context, DRS measurements on aqueous solutions of the more soluble K_2ox would be of interest.

At infinite dilution, $Z_s(OAc^-) \approx 11$ at 25 °C, which is about double of that of formate (Figure 6), and although $Z_s(OAc^-)$ decreases linearly with increasing c, it always remains greater than $Z_s(OFm^-)$. Similarly, $Z_{ib}(OAc^-) > Z_{ib}(OFm^-)$ over the entire concentration range (Figure 5), which means that $Z_t(OAc^-) > Z_t(OFm^-)$ at all concentrations, with the difference becoming smaller at higher c. These observations are consistent with a significant contribution of the methyl group to the hydration of OAc^-. There are three plausible explanations of this contribution: (1) increased hydrophilic hydration of the $-COO^-$ moiety due to the electron donating effect of the $-CH_3$ group; (2) semihydrophilic hydration[56] of the $-CH_3$ moiety, as a result of the polarization of the C−H bonds by the carboxylate group; or (3) hydrophobic hydration of $-CH_3$.[29,57−59]

Recent QM/MM simulations of OAc^-−water interactions in aqueous solution suggest[47] that semihydrophilic hydration of $-CH_3$ is unlikely; rather, a repulsive interaction seems to operate. Similarly, theoretical calculations[60] based on the partial-equalization-of-orbital-electronegativity method suggest only a slight increase of negative charge on the oxygen atoms in OAc^- compared to those in OFm^-, so the electron donating effect of $-CH_3$ also cannot explain the difference between $Z_s(OAc^-)$ and $Z_s(OFm^-)$. It follows that this difference must be due to the hydrophobicity of the $-CH_3$ group in OAc^-. This conclusion is consistent with the computer simulations and theoretical considerations of Laage et al.[57] who found that water molecules adjacent to hydrophobic moieties are retarded by a factor of ∼1.5 compared to bulk water.

The existence of hydrophobic hydration of the methyl group in OAc^- contrasts markedly with the behavior observed for the methyl groups in, for example, tetramethylammonium bromide (TMAB) for which no slow water was detected.[29] This implies that the hydrophobic hydration of methyl groups is significantly affected by their structural/chemical environment: in TMAB, the $-CH_3$ groups are directly attached to a slightly hydrophilic cationic center, whereas in OAc^-, the $-CH_3$ group is slightly separated from a strongly hydrophilic anionic center. Further systematic studies will be necessary to clarify this potentially important issue.

4.4. Temperature Dependence of Ion Hydration in NaOAc(aq). Typical DR spectra obtained for NaOAc(aq) at various temperatures are given in Figures S1 to S3, Supporting Information. As already noted, the $\varepsilon''(\nu)$ curves show a clear shift in position toward lower frequencies with increasing c at all investigated temperatures. However, with increasing temperature (Figure S4b, Supporting Information) the $\varepsilon''(\nu)$ curves shift toward higher frequencies, and the apparent amplitude decreases.

The amplitudes of the two water-related processes, $S_b = \varepsilon_3(c) - \varepsilon_\infty$ (Figure S9, Supporting Information) and S_s (Figure S10, Supporting Information), were used to calculate Z_{ib} and Z_s for NaOAc(aq) at 15 and 35 °C, following the procedure described in section 4.3. Figure S11 (Supporting Information) shows Z_{ib} for NaOAc(aq), as a function of c at different temperatures. The values of $Z_{ib}(Na^+)$ used to estimate $Z_{ib}(OAc^-)$ are given in Figure S12 of the Supporting Information. The $Z_{ib}(Na^+)$ values at 25 °C (as already noted) and 35 °C were obtained by reanalysing literature data for NaCl(aq)[19] with eq 5. Since suitable data were not available at 15 °C, the DR spectra of NaCl(aq) were recorded at this temperature in the frequency range $0.2 \le \nu(\mathrm{GHz}) \le 50$ and analyzed with eq 5.

At low concentrations, $Z_s(OAc^-)$ strongly decreases with increasing temperature (Figure 6), consistent with increased thermal motion. However, at high concentrations, the effect of temperature is much diminished (Figure 6), but the effective number of irrotationally bound water molecules, $Z_{ib}(OAc^-)$, seems to increase with increasing temperature (Figure S11, Supporting Information), which is opposite to the usual[19] trend (as was also found with respect to concentration, section 4.4).

The overall picture that emerges from Figures 6 and S11 (Supporting Information) is that temperature-induced dehydration of acetate ions becomes less effective with increasing solute concentration, such that close to saturation, the Z_s values become almost independent of temperature. Additionally, the already weak thermal dehydration effect for slow water at high c is partly counteracted by the increase of Z_{ib} (Figure S11, Supporting Information) so that at the highest c(NaOAc), the total hydration number, $Z_t(OAc^-)$, is almost independent of temperature, being ∼6.3, ∼6.2, and ∼5.4 at 15, 25, and 35 °C, respectively. Since these values are also close to the concentration-independent total hydration number of formate, $Z_t(OFm^-) \approx 5.2$, it can be concluded that the data for the highest acetate concentration represents $Z_t(-COO^-)$. This also suggests that the hydrophobic hydration of the $-CH_3$ moiety in OAc^- rapidly breaks down with increasing c and T. Although the present spectra provide no direct evidence, it may be speculated that this decrease of Z_s might be accompanied by some sort of aggregation of the hydrophobic methyl groups similar to that found previously for large hydrophobic ions.[29,30]

4.5. Bulk Water Dynamics. Over the investigated concentration range for NaOFm(aq), the relaxation time of bulk water, τ_b, decreases by almost 30% at 25 °C (Figure S7, Supporting Information). For NaOAc(aq) at the same temperature (Figure S8a, Supporting Information), the concentration-induced decrease is less pronounced (∼13% over the investigated temperature range) but consistent with the exponential increase of τ_b in pure water, the bulk-water relaxation time increases strongly with decreasing temperature. These two effects (Figures S7 and S8a, Supporting Information), indicate that the solute influences not only those water molecules close to the ions (i.e., in the first hydration shell), as has been claimed on the basis of time-resolved infrared studies,[61] but also the bulk water dynamics. Similar findings have been reported in dielectric[11] and neutron diffraction studies[62] of other electrolytes in aqueous solution.

The temperature dependence of τ_b can be analyzed in terms of the Eyring equation

$$\ln \tau = \ln \frac{h}{k_B T} - \frac{\Delta S^\ddagger}{R} + \frac{\Delta H^\ddagger}{RT} \qquad (12)$$

where h is Planck's constant, R is the universal gas constant, and $\Delta S^\ddagger$ and $\Delta H^\ddagger$ are, respectively, the activation entropy and activation enthalpy. Application of eq 12 to the bulk water relaxation time in Table S2 (Supporting Information) reveals (Figure 7) that $\Delta H^\ddagger$ is nearly constant at ∼15 kJ mol^{-1} at low c

dx.doi.org/10.1021/jp207504d | J. Phys. Chem. B 2012, 116, 314–323

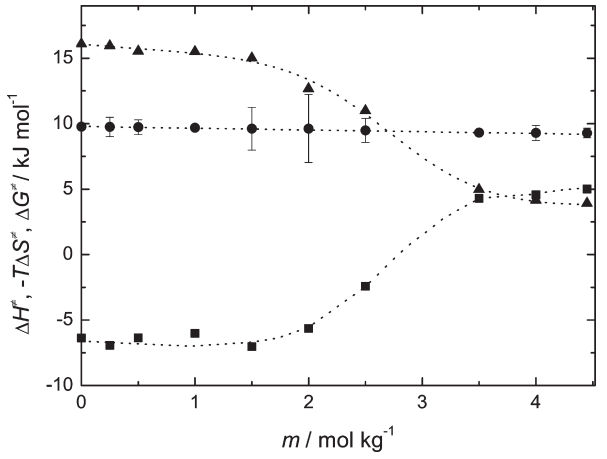

Figure 7. Concentration dependence of the activation parameters, $\Delta H^{\ddagger}$ (▲), $-T\Delta S^{\ddagger}$ (■, T = 298.15 K), and $\Delta G^{\ddagger}$ (●) of the bulk-water relaxation time, τ_b, in NaOAc(aq). Dotted lines are included only as a visual guide.

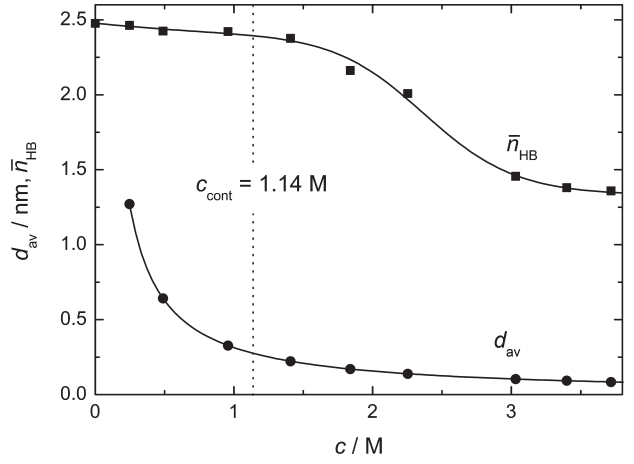

Figure 8. Concentration dependence of the average number of hydrogen bonds per bulk-water molecule, $\bar{n}_{HB}$, and the average distance between the hydrated cations and anions, d_{av}, in NaOAc(aq). The dotted line indicates c_{cont}, the concentration at which the hydration spheres of the cations and the anions start overlapping.

but drops significantly at $c \gtrsim 1.5$ M to ~5 kJ mol^{-1}. Over approximately the same concentration range, $\Delta S^{\ddagger}$ changes sign from ca. +20 J K^{-1} mol^{-1} at low c to −16 J K^{-1} mol^{-1}, corresponding to $-T\Delta S^{\ddagger}$ changing from ca. −6 kJ mol^{-1} to +5 kJ mol^{-1} (Figure 7).

The most interesting feature of Figure 7 is that as long as the average distance between the centers of the hydrated cations and anions,[63] d_{av} (nm) = 0.94 × $[c/\mathrm{M}]^{-1/3}$, is relatively large, the magnitudes of $\Delta S^{\ddagger}$ and $\Delta H^{\ddagger}$ are similar to those of pure water (20.4 ± 0.7 J K^{-1} mol^{-1} and 15.9 ± 0.2 kJ mol^{-1}, respectively, at 25 °C).[29] At higher concentrations, roughly where d_{av} is less than the contact distance of the hydrated cations and anions, both $\Delta H^{\ddagger}$ and $\Delta S^{\ddagger}$ change rapidly but in opposite directions. Obviously, the structure and dynamics of whatever bulk water remains at these high solute concentrations differ significantly from those in dilute solutions. The negative values for $\Delta S^{\ddagger}$ at c > 3 M suggest that in these concentrated solutions water reorientation must be highly cooperative, possibly because of the increasing confinement and isolation of the remaining bulk water pools between the hydrated ions.[64]

Assuming for simplicity that only water molecules with (at most) a single H-bond can reorient, the average number of hydrogen bonds formed by the bulk water molecules can be estimated[29,65] as

$$\bar{n}_{HB} = \frac{\Delta H^{\ddagger}}{\Delta_{HB}H} + 1 \qquad (13)$$

where $\Delta_{HB}H$ = 10.9 ± 0.4 kJ mol^{-1} is the strength of the H_2O-H_2O hydrogen bond in the pure water.[66] As can be seen in Figure 8, $\bar{n}_{HB}$ remains close to the bulk-water value, 2.48,[67] up to ~1.5 M but then decreases considerably, indicating a highly disrupted water structure at high solute concentrations.

Surprisingly, the Gibbs energy of activation, calculated as $\Delta G^{\ddagger} = \Delta H^{\ddagger} - T\Delta S^{\ddagger}$, shows (Figure 7) a pronounced enthalpy−entropy compensation (EEC) effect, which keeps $\Delta G^{\ddagger}$ almost constant over the entire concentration range. The occurrence of this EEC effect in the kinetic domain is interesting because such effects have mostly been observed for thermodynamic quantities, where their significance (or otherwise) has been much disputed.[68]

A similar analysis of the slow-water relaxation time, τ_s, would be of considerable interest.[29,69] Unfortunately, as mentioned in section 4.2, this is not possible because τ_s cannot be easily extracted from the experimentally determined τ_{comp}.

5. CONCLUSIONS

The present DR spectra have shown that both OFm^- and OAc^- are reasonably well hydrated in aqueous solution. However, unlike simple inorganic ions such as CO_3^{2-}, which freeze (irrotationally bind) water molecules, both these carboxylate ions essentially just slow down the dynamics of the water molecules in their first hydration shell, with only 1 or 2 water molecules becoming completely immobilized on the DRS time scale. The much greater number of slow water molecules around each anion arises from two sources: hydrophilic interaction with the $-COO^-$ moiety and hydrophobic hydration of the $-CH_3$ group in OAc^-. While the former is largely unaffected by solute concentration and temperature, the latter is fragile, decreasing markedly with increasing concentration (solute−solute interactions) and temperature (thermal motions).

There is some indication for very weak association between Na^+ and both OAc^- and OFm^- in aqueous solution, but the effects were too small for quantitative analysis. For NaOAc(aq), the activation enthalpy and entropy of the bulk-water relaxation suggested major changes in structure and dynamics. Possibly, this is because of the formation of isolated bulk water pools with restricted H-bonding confined to the interstices remaining between the hydrated ions at high solute concentrations.

■ ASSOCIATED CONTENT

Supporting Information. Densities, electrical conductivities, limiting permittivities, relaxation times, and reduced error function values for NaOFm and NaOAc; spectra of relative permittivity and dielectric loss of NaOAc at different temperatures and concentrations; relaxation time distribution functions of NaOFm and NaOAc; and concentrations dependence plots. This material is available free of charge via the Internet at http://pubs.acs.org.

AUTHOR INFORMATION

Corresponding Author
*E-mail: Richard.Buchner@chemie.uni-regensburg.de.

ACKNOWLEDGMENT

We thank W. Kunz for the provision of laboratory facilities at Regensburg, and S. Schrödle for recording VNA data at Murdoch University, Australia. The Higher Education Commission (HEC) of Pakistan is gratefully acknowledged for funding H.M.A.R.'s stay in Germany. This work was funded by the Deutsche Forschungsgemeinschaft.

REFERENCES

(1) Bellisent-Funel, M.-C., Ed. *Hydration Processes in Biology*; IOS Press: Dordrecht, The Netherlands, 1998.
(2) Halle, B.; Denisov, V. P. *Methods Enzymol.* **2001**, *338*, 178.
(3) Sasisanker, P.; Weingärtner, H. *ChemPhysChem* **2008**, *9*, 2802.
(4) Oleinikova, A.; Sasisanker, P.; Weingärtner, H. *J. Phys. Chem. B* **2004**, *108*, 8467.
(5) Modig, K.; Liepinsh, E.; Otting, G.; Halle, B. *J. Am. Chem. Soc.* **2004**, *126*, 102.
(6) Liang, T.; Walsh, T. R. *Phys. Chem. Chem. Phys.* **2006**, *8*, 4410.
(7) Xu, H.; Berne, B. J. *J. Phys. Chem. B* **2001**, *105*, 11929.
(8) Kameda, Y.; Sugawara, K.; Usuki, T.; Uemura, O. *Bull. Soc. Chem. Jpn.* **2003**, *76*, 935.
(9) McLain, S. E.; Soper, A. K.; Terry, A. E.; Watts, A. *J. Phys. Chem. B* **2007**, *111*, 4568.
(10) Buchner, R. *Pure Appl. Chem.* **2008**, *80*, 1239.
(11) Buchner, R.; Hefter, G. *Phys. Chem. Chem. Phys.* **2009**, *11*, 8984.
(12) Wyttenbach, T.; Bowers, M. G. *Chem. Phys. Lett.* **2009**, *480*, 1.
(13) Beveridge, A. J.; Heywood, G. C. *Biochemistry* **1993**, *32*, 3325.
(14) Lileev, A. S.; Balakaeva, I. V.; Lyashchenko, A. *J. Mol. Liq.* **2000**, *87*, 11.
(15) Longinova, D. V.; Lileev, A. S.; Lyashchenko, A. K.; Khar'kin, V. S. *Russ. J. Inorg. Chem.* **2003**, *48*, 278.
(16) Longinova, D. V.; Lileev, A. S.; Lyashchenko, A. K.; Aladko, L. *J. Non-Cryst. Solids* **2005**, *351*, 2882.
(17) Lide, D. R., Ed. *CRC-Handbook of Chemistry and Physics*, 85th ed.; CRC Press: Boca Raton, FL, 2004.
(18) Stoppa, A.; Hunger, J.; Buchner, R. *J. Chem. Eng. Data* **2009**, *54*, 472.
(19) Buchner, R.; Hefter, G. T.; May, P. M. *J. Phys. Chem. A* **1999**, *103*, 1.
(20) Barthel, J.; Buchner, R.; Eberspächer, P. N.; Münsterer, M.; Stauber, J.; Wurm, B. *J. Mol. Liq.* **1998**, *78*, 83.
(21) Böttcher, C. F. J.; Bordewijk, P. *Theory of Electrical Polarization*, 2nd ed.; Elsevier: Amsterdam, The Netherlands, 1978; Vol. 2.
(22) Kremer, F.; Schönhals, A. *Broadband Dielectric Spectroscopy*; Springer: Berlin, Germany, 2003.
(23) Note that eq 2 corrects the total sample response only for dc conductivity, i.e., for steady-state ion migration. Possible frequency-dependent effects associated with ionic motion will contribute to the complex permittivity spectrum, $\hat{\varepsilon}(\nu)$.
(24) Fukasawa, T.; Sato, T.; Watanabe, J.; Hama, Y.; Kunz, W.; Buchner, R. *Phys. Rev. Lett.* **2005**, *95*, 197802.
(25) Bevington, P. R. *Data Reduction and Error Analysis for the Physical Sciences*; McGraw-Hill: New York, 1978.
(26) Buchner, R.; Chen, T.; Hefter, G. *J. Phys. Chem. B* **2004**, *108*, 2365.
(27) Zasetsky, A. Y.; Buchner, R. *J. Phys.: Condens. Matter* **2011**, *23*, 025903.
(28) Note that at low c, τ_1 for NaOFm(aq) and τ_2 for NaOAc(aq) were fixed to their average values to reduce the scatter of the corresponding amplitudes.
(29) Buchner, R.; Hölzl, C.; Stauber, J.; Barthel, J. *Phys. Chem. Chem. Phys.* **2002**, *4*, 2169.
(30) Wachter, W.; Buchner, R.; Hefter, G. *J. Phys. Chem. B* **2006**, *110*, 5147.
(31) Fedotova, M. V.; Kruchinin, S. E.; Rahman, H. M. A.; Buchner, R. *J. Mol. Liq.* **2011**, *159*, 9.
(32) Tromans, A.; May, P. M.; Hefter, G.; Sato, T.; Buchner, R. *J. Phys. Chem. B* **2004**, *108*, 13789.
(33) Wachter, W.; Buchner, R.; Hefter, G. To be submitted for publication.
(34) Serr, A.; Netz, R. R. *Int. J. Quantum Chem.* **2006**, *106*, 2960.
(35) Bončina, M.; Apelblat, A.; Bešter-Rogač, M. *J. Chem. Eng. Data* **2010**, *55*, 1951.
(36) Jagoda-Cwiklik, B.; Vácha, R.; Lund, M.; Srebro, M.; Jungwirth, P. *J. Phys. Chem. B* **2007**, *111*, 14077.
(37) Schrödle, S. Effects of Nonionic Surfactants and Related Compounds on the Cooperative and Molecular Dynamics of their Aqueous Solutions. Ph.D. Thesis, University of Regensburg, Regensburg, Germany, 2005.
(38) Hefter, G. T. *J. Solution Chem.* **1984**, *13*, 179.
(39) Partanen, J. I. *Acta Chem. Scand.* **1998**, *52*, 985.
(40) Barthel, J.; Hetzenauer, H.; Buchner, R. *Ber. Bunsenges. Phys. Chem.* **1992**, *96*, 1424.
(41) Hubbard, J. B.; Onsager, L. *J. Chem. Phys.* **1977**, *67*, 4850. (b) Hubbard, J. B. *J. Chem. Phys.* **1978**, *68*, 1649. (c) Hubbard, J. B.; Colonomos, P.; Wolynes, P. G. *J. Chem. Phys.* **1979**, *71*, 2652.
(42) Strictly, additivity is applicable only at infinite dilution, but given the approximate nature of these calculations and consistency with previous experience,[10,19,11] it continues to hold reasonably well at finite concentrations.
(43) Wachter, W.; Kunz, W.; Buchner, R.; Hefter, G. *J. Phys. Chem. A* **2005**, *109*, 8675.
(44) Buchner, R.; Capewell, S. G.; Hefter, G.; May, P. M. *J. Phys. Chem. B* **1999**, *103*, 1185.
(45) Payaka, A.; Tongraar, A.; Rode, B. M. *J. Phys. Chem. A* **2009**, *113*, 3291.
(46) Sterpone, F.; Stirnemann, G.; Hynes, J. T.; Laage, D. *J. Phys. Chem. B* **2010**, *114*, 2083.
(47) Payaka, A.; Tongraar, A.; Rode, B. M. *J. Phys. Chem. A* **2010**, *114*, 10443 and references cited therein.
(48) Leung, K.; Rempe, S. B. *J. Am. Chem. Soc.* **2004**, *126*, 344.
(49) Kameda, Y.; Mori, T.; Nishiyama, T.; Usuki, T.; Uemura, O. *Bull. Soc. Chem. Jpn.* **1996**, *69*, 1495.
(50) Kameda, Y.; Fukahara, K.; Mochiduki, K.; Naganuma, H.; Usuki, T.; Uemura, O. *J. Non-Cryst. Solids* **2002**, *312*−*314*, 433.
(51) Kameda, Y.; Ebata, H.; Usuki, T.; Uemura, O.; Misawa, M. *Bull. Soc. Chem. Jpn.* **1994**, *67*, 3159.
(52) Naganuma, H.; Kameda, Y.; Usuki, T.; Uemura, O. *J. Phys. Soc. Jpn. Suppl. A* **2001**, *70*, 356.
(53) Kuntz, I. D. *J. Am. Chem. Soc.* **1971**, *93*, 514.
(54) Fedotova, M. V.; Kruchinin, S. E. *J. Mol. Liq.* **2011**, *164* (3), 201–206.
(55) Buchner, R.; Samani, F.; May, P. M.; Sturm, P.; Hefter, G. *Chem. Phys. Chem.* **2003**, *4*, 373.
(56) Backlund, S.; Eriksson, F.; Friman, R.; Rundt, K.; Sjöblom, J. *Acta Chem. Scand.* **1980**, *34*, 381.
(57) Laage, D.; Stirnemann, G.; Hynes, J. T. *J. Phys. Chem. B* **2009**, *113*, 2428.
(58) Luzar, A. *Faraday Discuss. Chem. Soc.* **1996**, *103*, 29.
(59) Laage, D.; Hynes, J. T. *J. Phys. Chem. B* **2008**, *112*, 14230.
(60) No, K. T.; Grant, A.; Jhon, M. S.; Scheraga, H. A. *J. Phys. Chem.* **1990**, *94*, 4740.
(61) Bakker, H. J. *Chem. Rev.* **2008**, *108*, 1456.
(62) Mancinelli, R.; Botti, A.; Bruni, F.; Ricci, M. A.; Soper, A. K. *Phys. Chem. Chem. Phys.* **2007**, *9*, 2959.
(63) Marcus, Y. *J. Solution Chem.* **2009**, *38*, 513.
(64) Turton, D. A.; Hunger, J.; Hefter, G.; Buchner, R.; Wynne, K. *J. Chem. Phys.* **128**, *2008*, 161102.

(65) Buchner, R.; Barthel, J.; Stauber, J. *Chem. Phys. Lett.* **1999**, *306*, 57.
(66) Walrafen, G. E.; Fisher, M. R.; Hokmabadi, M. S.; Yang, W.-H. *J. Chem. Phys.* **1986**, *85*, 6970.
(67) The value for pure water, $\bar{n}_{HB} = 2.48$,[65] is supported by various data from other methods.[71−73]
(68) Hefter, G.; Marcus, Y.; Waghorne, W. E. *Chem. Rev.* **2002**, *102*, 2773 and references cited therein.
(69) Schrödle, S.; Hefter, G.; Kunz, W.; Buchner, R. *Langmuir* **2006**, *22*, 924.
(70) Error bars for Z_{ib} were calculated for each temperature from the standard deviations of fits of the polynomial $S_b(c) = S_b(0) - a_1c + a_2c^{3/2}$ to the experimental bulk-water amplitudes, with $S_b(0)$ fixed to the corresponding pure-water value of ref 37. Error bars for Z_s were obtained from the standard deviations of $S_s(c) = a_1c + a_2c^{3/2}$.
(71) Hawlicka, E.; Dlugoborski, T. *Chem. Phys. Lett.* **1997**, *268*, 325.
(72) Bertolini, D.; Cassettari, M.; Ferrario, M.; Grigolini, P.; Salvetti, G. *Adv. Chem. Phys.* **1985**, *62*, 277.
(73) Wernet, P.; Nordlund, D.; Bergmann, U.; Cavalleri, M.; Odelius, M.; Ogasawara, H.; Näslund, L. Å.; Hirsch, T. K.; Ojamäe, L.; Glatzel, P.; Pettersson, L. G. M.; Nilsson, A. *Science* **2004**, *304*, 995.